

Mechanism and Scalability in Resistive Switching of Metal-Pr_{0.7}Ca_{0.3}MnO₃ Interface

S. Tsui, Y. Q. Wang, and Y. Y. Xue

*Department of Physics and Texas Center for Superconductivity,
University of Houston, 202 Houston Science Center, Houston, Texas 77204-5002*

C. W. Chu

*Department of Physics and Texas Center for Superconductivity,
University of Houston, 202 Houston Science Center, Houston,
Texas 77204-5002; Lawrence Berkeley National Laboratory, 1 Cyclotron Road, Berkeley,
California 94720; and Hong Kong University of Science and Technology, Hong Kong*

(Dated: October 11, 2018)

The polarity-dependent resistive-switching across metal-Pr_{0.7}Ca_{0.3}MnO₃ interfaces is investigated. The data suggest that shallow defects in the interface dominate the switching. Their density and fluctuation, therefore, will ultimately limit the device size. While the defects generated/annihilated by the pulses and the associated carrier depletion seem to play the major role at lower defect density, the defect correlations and their associated hopping ranges appear to dominate at higher defect density. Therefore, the switching characteristics, especially the size-scalability, may be altered through interface treatments.

The renewed interest in various resistive switching phenomena is largely driven by recent market demands for nano-sized nonvolatile memory devices.¹ While the current boom of consumer electronics may largely be attributed to the successful miniaturization of both FLASH chips and mini hard drives, cheaper and smaller devices are called for. Various resistive hysteretic phenomena are consequently studied with the hope that the size limitations associated with the related physics/chemistry/technology might be less severe.² Our limited knowledge about the mechanisms so far, however, makes the evaluation difficult. This is especially true for the switching across metal-Pr_{0.7}Ca_{0.3}MnO₃ (PCMO) interfaces.^{3,4,5,6} Several models, *i.e.* bulk phase-separation,³ carrier-trapping in pre-existing metallic domains,^{7,8} and field-induced lattice defects,⁴ have been proposed. Each possesses its own distinguishable size-limitation, *e.g.* the statistics of the associated local mesostructures. Here, we report our mechanism investigation through both the trapped-carrier distribution and their hopping range. Our data suggest that the characteristics may largely be engineered through the mesostructure of the interfacial defects.

Bulk PCMO, in great contrast with well known semiconductors, has a rather high nominal carrier concentration with its high resistivity mainly attributed to hopping barriers.⁹ Local defects, therefore, appear as a natural cause of the resistive switching. Following this line of reasoning, a domain model has recently attracted much attention.^{7,8} There, a tunneling from the electrode to some pre-existing interfacial metallic domains has been assumed to be the dominant process. Consequently, the carrier-occupation in the domains may change with the carrier-trapping during the write pulses, and cause the *R*-switch between an on (low resistance) and an off (high resistance) state. This is realized through either the change of the tunneling probability⁷ or a doping-induced metal-insulator transition.⁸ Useful devices based on this mech-

anism, therefore, should typically be much larger than these interfacial domains. It is interesting to note that even if the “domains” can be reduced to individual lattice defects (or small clusters) as in the proposed defect modification model,⁴ the fluctuation (inhomogeneity) of the defect density still sets a limit for the size scalability just like the dopant fluctuation in Si nano-devices.¹⁰ The defect (domain) density, therefore, requires exploration, and the interfacial capacitance, $C(\omega)$, can serve to distinguish between these models.

While the domain model may simulate very divergent dc $I - V$ characteristics by adjusting the fitting parameters,⁷ the measured capacitance is expected to be ω -independent with $C_{on} = C_{off}$ ($C_{on} > C_{off}$) for tunneling-probability (metal-insulator transition) scenarios, where C_{on} and C_{off} are $C(\omega)$ in the on and off states, respectively. In the defect modification model, however, the $C(\omega)$ measures the net trapped carriers in the interface, *i.e.* with $R_{off}/R_{on} \approx C_{off}/C_{on}$ in the space-charge-limited-current (SCLC) region, where R_{on} and R_{off} are $R(\omega)$ in the on and off states, respectively. It should be noted that the carriers trapped behind a hopping barrier V_{hop} respond to a step-disturbance as $\exp[-v_0 t \cdot \exp(-V_{hop}/k_B T)]$. Therefore, $C(\omega) \propto \int_{\omega}^{\infty} k_B T [dN/dV_{hop}]/\omega d\omega$, *i.e.* the density of states (DOS) at the Fermi level for the defects with the hopping barrier lower than $V_{hop} = k_B T \ln(v_0/\omega)$, where k_B and $v_0 \approx 10^{12}$ sec⁻¹ are the Boltzmann constant and the trial frequency, respectively. An experimental challenge, however, exists in separating the interfacial $C(\omega)$ from the bulk contribution. We have previously reported a preliminary result for an Ag-PCMO interface⁴ through the traditional Cole-Cole procedure, which assumes that all C 's and R 's are ω -independent, under a standard two-leads measurement configuration. In the SCLC region, the observed $C_{off} = 2.2$ nF and $C_{on} = 1.6$ nF clearly contradict the domain model but qualitatively agree with the defect

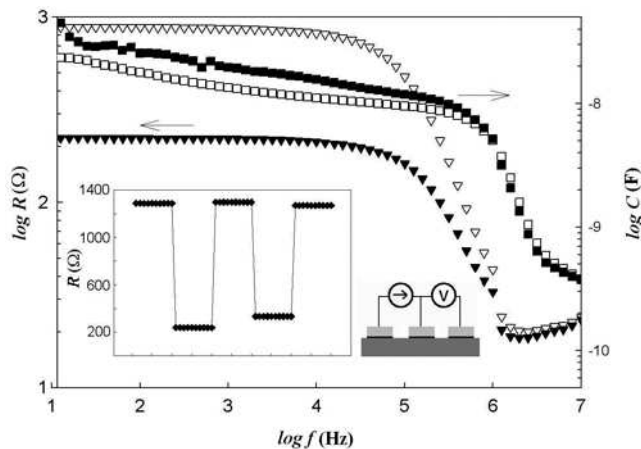


FIG. 1: $R(\omega)$ (triangle symbols) and $C(\omega)$ (square symbols) of a Au-PCMO setup at on- (solid) and off- (open) states. Bottom left inset: the switching series. Bottom right inset: three-lead setup.

modification model. The data, however, also raise a serious concern about the size-limitation. In a sense, the observed $C/q \approx 10^{12}$ electrons/cm², where $q = 1.6 \cdot 10^{-19}C$ is the electron charge, is a measure of the trapped carriers (or the shallow defects near the Fermi level), and puts a statistical size-limit on the order of 10–100 nm if the switching is due to a change in defect density. Therefore, a possible route to further minimizing the device size would be to increase the $C(\omega)$. A dilemma, however, arises: denser shallow defects would also enhance the thermal excitation. Across a $C(\omega)$ threshold, the SCLC may not be reachable, and the denser defects at the off states, functioning as donors, might even enhance the conductivity. It is therefore even unclear whether samples with a much larger $C(\omega)$ are switchable.

We finally found several metal electrode-PCMO film configurations, with the low- ω interfacial $C > 100$ nF/mm², a value one order of magnitude higher, although the conditions for reproducibly synthesizing such samples are not yet clear. Repeatable switching has been obtained (bottom left inset, Fig. 1). The Cole-Cole plot, however, shows that the C_{off}/C_{on} is even smaller than 1, while $R_{off}/R_{on} > 2$, a scenario closer to the domain model. To explore the issue, a new procedure is developed to directly measure the complex interfacial admittance $1/R(\omega) - i\omega C(\omega)$. This is done by extending the previous three-leads R -measurement to the off-phase part through a Solartron SI 1260 impedance/gain-phase analyzer (bottom right inset, Fig. 1). Resistors/capacitors networks were used to verify that the phase uncertainty is less than 0.1°. Both $R(\omega)$ and $C(\omega)$ of the interface, therefore, can be accurately deduced over 10^2 – 10^7 Hz.

The $C(\omega)$ and the $R(\omega)$ observed undergo a step-like jump over a narrow range of 0.1 and 3 MHz, with the C -jump occurring at higher ω (Fig. 1). This is similar to the Maxwell-Wagner relaxation,¹¹ but differs from dielectric Debye relaxation.¹² Carrier polarization, *i.e.*

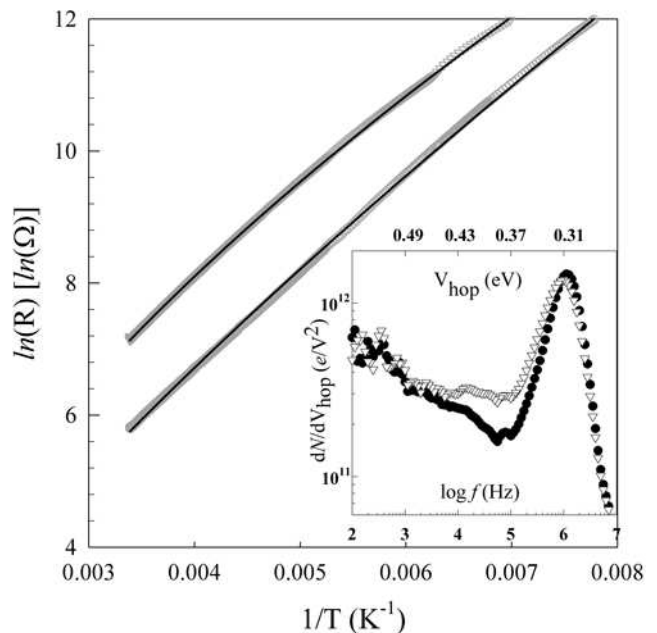


FIG. 2: $R(T)$ between 150 and 300 K. Top (bottom) grey symbols: data at off- (on-) states. Lines: VRH fits. Inset: the calculated defect distribution in the 0.1 mm² interface layer. Open triangles: the on state. Solid circles: the off state.

trapping and hopping in disordered solids,¹³ appears to be a natural interpretation. In such models, only the hopping paths with all barriers $V_{hop} \ll k_B T \ln(\omega/v_0)$ contribute to the apparent conductivity $1/R(\omega)$, and the $\omega dC(\omega)/d\omega$ measures the defect distribution against the hopping barriers, dN/dV_{hop} , at the Fermi level. The jumps (Fig. 1), therefore, suggest a defect mesostructure with many short conducting clusters (domains) with the intra-cluster $V_{hop} < 0.3$ eV separated by slightly higher inter-cluster barriers, *i.e.* around 0.4 eV (inset, Fig. 2). It is interesting to note that the R_{on} and R_{off} are distinct, *i.e.* switchable, below 0.1–1 MHz, but the corresponding dN/dV_{hop} is practically the same as indicated by the Cole-Cole plot. This is very different from the samples with smaller $C(\omega)$, although both show higher R after positive pulses. Also, the same $R(\omega)$ above 1 MHz at both on and off states indicates a limitation on the read speed in future potential applications.

It should be pointed out that such strong dispersions of $R(\omega)$ and $C(\omega)$ suggest that the domain model is also in disagreement with the data. The interfacial hopping in the model has been attributed to a *single* barrier layer between the electrode and the proposed interfacial domain, and should therefore be ω -independent for $\omega \ll v_0$. Thus, a more complicated defect network should be invoked to accommodate the dispersions. It is also interesting to note that the thermo-produced carriers can be directly deduced from the $C(\omega)$ observed. The calculated value, $> 10^{17}$ sec⁻¹ below 100 kHz within the interfacial layer, is far higher than the reported injected current, $\leq 5 \cdot 10^{14}$

sec^{-1} , at the SCLC region.⁴ This supports the above discussion for samples with large $C(\omega)$, and suggests that the switching mechanism can be modified through interface engineering.

To answer the key question of why the switching can still occur, $R(T)$ was measured at both on- and off-states (Fig. 2). While the $R(T)$'s appear to be almost parallel, which makes the switching difficult to understand if $C_{\text{off}} \approx C_{\text{on}}$, a closer examination shows that $R = a \cdot T \cdot \exp[-(T_0/T)^\gamma]$ in the variable-range-hopping (VRH) formulation might be a better description, as suggested by the slight curvatures in Fig. 2. For this particular sample, the fitting parameters are $\gamma = 0.85$ (0.61) and $T_0 = 2089$ K (8353 K) for the on (off) states, respectively. The γ and T_0 are traditionally associated with $1/(1+d)$ and $1/\text{DOS}$, where d is the dimensionality.¹⁴ The changes in both γ and T_0 , therefore, tentatively suggest that the arrangement of the defect-structures are changed. The switching, in such a case, might be more about the local structure than the average defect density.

To verify this assumption, the small-signal ac $R(\omega)$ at various dc biases and temperatures was measured (inset, Fig. 3). The normalized $I-V$ characteristics between 8 and 55 °C are scaled into a single trace as suggested by Mott's formula of $R/R(E=0) \propto \exp(-l \cdot E/k_B T)^\gamma$ or $\exp(-l \cdot E/k_B T)$,¹⁵ where l and E are the hopping range and the electric field, respectively. The physical picture, *i.e.* the longer the hopping range, the larger the field effects will be, is straightforward and independent of the hopping details, although the absolute value may be affected by the 10 nm assumed thickness⁴ of the interfacial layer. Our data, therefore, demonstrate that the hopping range is longer at the off state for $\omega < 1$ MHz. It is also interesting to note the unusually small l for $\omega > 1$ MHz (Fig. 1, 3). This may appear only if the associated hopping barriers are negligible, which is further suggestive of local defect mesostructure. With high enough defect density, the formation of local defect-correlations becomes a means to modify the switching performance. It should be noted that, in order to accommodate the observed $C_{\text{off}}/C_{\text{on}}$, the conductance may be dominated by only a few percolation paths, such that simply enhancing $C(\omega)$ may not necessarily reduce the size limitations. Direct observations of such structures are called for and planned.

In conclusion, we have shown that the interfacial resistive switch found in metal-PCMO systems is a defect-mediated process. Whereas a defect density alteration occurs in samples with $C(\omega < 10^5 \text{ Hz}) \leq 100 \text{ nF/mm}^2$, we propose that the change in defect mesostructure may

cause switching in the samples with larger $C(\omega)$. Further investigation of the parameters controlling the defect distribution will shed light on how best to proceed with the nanoscaling and benchmarking of future device applications.

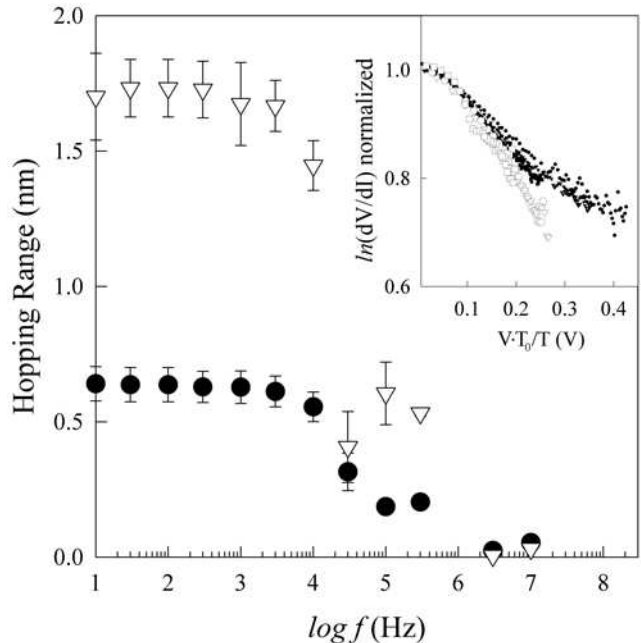


FIG. 3: Hopping range with respect to frequency for both off (open triangles) and on (solid circles) states. The switch is determined by low frequency inter-cluster hopping, whereas at high frequencies, percolative intra-cluster hopping occurs. Inset: raw $I-V$ data at several temperatures show the scaling of Mott's formula, where $T_0 = 300$ K.

Acknowledgments

The authors thank Prof. J. Miller and Dr. N. Nawarathna for the use of and technical assistance with the impedance analyzer. The work in Houston is supported in part by NSF Grant No. DMR-9804325, the T. L. L. Temple Foundation, the John J. and Rebecca Moores Endowment, the Robert A. Welch Foundation, and the State of Texas through the Texas Center for Superconductivity at the University of Houston; and at Lawrence Berkeley Laboratory by the Director, Office of Science, Office of Basic Energy Sciences, Division of Materials Sciences and Engineering of the U.S. Department of Energy under Contract No. DE-AC03-76SF00098.

¹ For example, P. Weiss, Science News **167**, 363 (2005).

² For example, R. Waser, Resistive Switching on SrTiO₃, Intel International Symposium on Resistive Switch Memory Device Benchmarking, 2005.

³ S. Q. Liu, N. J. Wu, and A. Ignatiev, Appl. Phys. Lett.

76, 2749 (2000).

⁴ A. Baikalov, Y. Q. Wang, B. Shen, B. Lorenz, S. Tsui, Y. Y. Sun, Y. Y. Xue, and C. W. Chu, Appl. Phys. Lett. **83**, 957 (2003); S. Tsui, A. Baikalov, J. Cmaidalka, Y. Y. Sun, Y. Q. Wang, Y. Y. Xue, C. W. Chu, L. Chen, and A. J.

- Jacobson, Appl. Phys. Lett. **85**, 317 (2004).
- ⁵ A. Sawa, T. Fujii, M. Kawasaki, and Y. Tokura, Appl. Phys. Lett. **85**, 4073 (2004).
- ⁶ A. Odagawa, H. Sato, I. H. Inoue, H. Akoh, M. Kawasaki, Y. Tokura, T. Kanno, and H. Adachi, Phys. Rev. B **70**, 224403 (2004).
- ⁷ M. J. Rozenberg, I. H. Inoue, and M. J. Sánchez, Phys. Rev. Lett. **92**, 178302 (2004).
- ⁸ M. J. Rozenberg, I. H. Inoue, and M. J. Sánchez, Appl. Phys. Lett. **88**, 033510 (2006); M. J. Rozenberg, I. H. Inoue, and M. J. Sánchez, Thin Solid Films **486**, 24 (2005); M. J. Rozenberg, I. H. Inoue, and M. J. Sánchez, cond-mat/0406646 (2004).
- ⁹ For example, H. Y. Hwang, S. W. Cheong, P. G. Radaelli, M. Marezio, and B. Batlogg, Phys. Rev. Lett. **75**, 914 (1995).
- ¹⁰ For example, J. D. Meindl, Q. Chen, and J. A. Davis, Science **293**, 2044 (2001).
- ¹¹ For example, Z. Yu and C. Ang, J. Appl. Phys. **91**, 794 (2002); P. Lunkenheimer, V. Bobnar, A. V. Pronin, A. I. Ritus, A. A. Volkov, and A. Loidl, Phys. Rev. B **66**, 052105 (2002).
- ¹² For example, A. K. Jonscher, IEEE Electrical Insulation Magazine **6**, 16 (1990).
- ¹³ J. C. Dyre and T. B. Schröder, Rev. Mod. Phys. **72**, 873 (2000).
- ¹⁴ For example, B. Sanjai, A. Raghunathan, T. S. Natarajan, G. Rangarajan, S. Thomas, P. V. Prabhakaran, and S. Venkatachalam, Phys. Rev. B **55**, 10734 (1997); V. I. Arkhipov, H. von Seggern, and E. V. Emelianova, Appl. Phys. Lett. **83**, 5074 (2003).
- ¹⁵ N. F. Mott and E. A. Davis, *Electronic Processes in Non-Crystalline Materials*, 2nd ed. (Clarendon, Oxford, 1979).